Space Sci Rev
DOI 10.1007/s11214-007-9153-y

Lunar Reconnaissance Orbiter Overview: The Instrument Suite and Mission

Gordon Chin · Scott Brylow · Marc Foote · James Garvin · Justin Kasper · John Keller · Maxim Litvak · Igor Mitrofanov · David Paige · Keith Raney · Mark Robinson · Anton Sanin · David Smith · Harlan Spence · Paul Spudis · S. Alan Stern · Maria Zuber

Received: 20 January 2007 / Accepted: 1 February 2007

Abstract NASA's Lunar Precursor Robotic Program (LPRP), formulated in response to the President's Vision for Space Exploration, will execute a series of robotic missions that will pave the way for eventual permanent human presence on the Moon. The Lunar Reconnaissance Orbiter (LRO) is first in this series of LPRP missions, and plans to launch in October of 2008 for at least one year of operation. LRO will employ six individual instruments to

G. Chin (✉) · J. Garvin · J. Keller · D. Smith
Goddard Space Flight Center, Greenbelt, MD 20771, USA
e-mail: gordon.chin-1@nasa.gov

S. Brylow
Malin Space Science Systems, San Diego, CA 92121, USA

M. Foote
Jet Propulsion Laboratory, California Institute of Technology, Pasadena, CA 91109, USA

J. Kasper · M. Zuber
Massachusetts Institute of Technology, Boston, MA 02139, USA

M. Litvak · I. Mitrofanov · A. Sanin
Russian Federal Space Agency Institute for Space Research, Moscow, 117997, Russia

K. Raney · P. Spudis
Applied Physics Laboratory, Johns Hopkins University, Baltimore, MD 20723, USA

M. Robinson
Arizona State University, Tempe, AZ 85287, USA

H. Spence
Boston University, Boston, MA 02215, USA

S.A. Stern
Southwest Research Institute, Boulder, CO 80302, USA

D. Paige
University of California, Los Angeles, CA 90095, USA

produce accurate maps and high-resolution images of future landing sites, to assess potential lunar resources, and to characterize the radiation environment. LRO will also test the feasibility of one advanced technology demonstration package. The LRO payload includes: Lunar Orbiter Laser Altimeter (LOLA) which will determine the global topography of the lunar surface at high resolution, measure landing site slopes, surface roughness, and search for possible polar surface ice in shadowed regions, Lunar Reconnaissance Orbiter Camera (LROC) which will acquire targeted narrow angle images of the lunar surface capable of resolving meter-scale features to support landing site selection, as well as wide-angle images to characterize polar illumination conditions and to identify potential resources, Lunar Exploration Neutron Detector (LEND) which will map the flux of neutrons from the lunar surface to search for evidence of water ice, and will provide space radiation environment measurements that may be useful for future human exploration, Diviner Lunar Radiometer Experiment (DLRE) which will chart the temperature of the entire lunar surface at approximately 300 meter horizontal resolution to identify cold-traps and potential ice deposits, Lyman-Alpha Mapping Project (LAMP) which will map the entire lunar surface in the far ultraviolet. LAMP will search for surface ice and frost in the polar regions and provide images of permanently shadowed regions illuminated only by starlight. Cosmic Ray Telescope for the Effects of Radiation (CRaTER), which will investigate the effect of galactic cosmic rays on tissue-equivalent plastics as a constraint on models of biological response to background space radiation. The technology demonstration is an advanced radar (mini-RF) that will demonstrate X- and S-band radar imaging and interferometry using light weight synthetic aperture radar. This paper will give an introduction to each of these instruments and an overview of their objectives.

Keywords Moon · Lunar · Vision for Space Exploration · NASA · Spacecraft · Space instrumentation · Remote observation

1 Introduction

The Lunar Reconnaissance Orbiter (LRO) is the first mission to be implemented in NASA's Lunar Precursor Robotic Program (LPRP), which aims to fulfill the President's Vision for Space Exploration. LRO is scheduled for an October 2008 launch date, and the mission will have a duration of 14 months, including a 2 month commissioning phase with the possibility of extended operations.

Six instruments were selected through a process of scientific peer review as well as technical, cost and management assessments. The selected instruments are the Lunar Orbiter Laser Altimeter (LOLA), the Lunar Reconnaissance Orbiter Camera (LROC), the Lunar Exploration Neutron Detector (LEND), the Diviner Lunar Radiometer Experiment (DLRE), the Lyman-Alpha Mapping Project (LAMP), and the Cosmic Ray Telescope for the Effects of Radiation (CRaTER). Section 2 provides a description of each of the selected instruments, as well as a description of how their measurement objectives are aligned with the goals of the LPRP.

Section 3 provides a description of the Mini Radio Frequency (Mini-RF) technology demonstration package, which was added after payload selection, in 2005.

Finally, Sect. 4 will give a brief description of the LRO spacecraft, instrument accommodations and baseline mission.

2 LRO Measurement Objectives and the Instrument Suite

In January 2004, the President of the United States announced a plan to advance the Nation's scientific, security, and economic interests through a space exploration program that integrates human and robotic exploration activities. This plan was documented by the *President's Space Exploration Policy Directive (NPSD31, Goal and Objectives)*, and *A Renewed Spirit of Discovery—The President's Vision for US Space Exploration (January 2004).* The specific actions required to carry out this new exploration program have been elaborated in the NASA response document "*The Vision for Space Exploration,*" dated February 2004.

NASA Headquarters subsequently established the following baseline Lunar Program Requirements:

1. Undertake lunar exploration activities to enable sustained human and robotic exploration of the Moon, Mars, and more distant destinations in the Solar System.
2. Starting no later than 2008, initiate a series of robotic missions to the Moon to prepare for and support future human exploration activities.
   a. Mission objectives shall include landing site identification and certification on the basis of potential resources.
   b. Measurements shall be made to support applied science and research relevant to the Moon as a step to Mars, to support engineering safety, and to determine engineering boundary conditions.
   c. Technology demonstrations and system testing shall be performed to support development activities for future human lunar and Mars missions.
3. Conduct the first extended human expedition to the lunar surface as early as 2015, but no later than the year 2020.
4. Use lunar exploration activities to further science and research.

The Lunar Reconnaissance Orbiter, under the Lunar Precursor Robotic Program, is the first step in achieving the goals set by NASA's "Vision for Space Exploration."

NASA also convened an external panel to assist in defining specific goals and measurement objectives needed for the initial steps in lunar robotic exploration. Based on recommendations of the panel, NASA issued an Announcement of Opportunity (AO) soliciting LRO investigations to provide the following high priority measurement sets:

- Characterization of the deep space radiation environment in lunar orbit, including neutron albedo, especially at energies in excess of 10 MeV, as well as:
  - Characterization of biological effects caused by exposure to the lunar orbital radiation environment.
  - Characterization of changes in the properties of multifunctional radiation shielding materials caused by extended exposure to the lunar orbital environment.
- Geodetic lunar global topography (at landing-site relevant scales).
- High spatial resolution hydrogen mapping of the Moon's surface.
- Temperature mapping in the Moon's polar shadowed regions.
- Landform-scale imaging of lunar surfaces in permanently shadowed regions.
- Identification of putative deposits of appreciable near-surface water ice in the Moon's polar cold traps.
- Assessment of meter and smaller-scale features to facilitate safety analysis for potential lunar landing sites.
- Characterization of the illumination environment in the Moon's polar regions at relevant temporal scales (i.e., in terms of hours).

In December 2004 NASA announced the selection of six instruments for LRO that will directly address all the measurement requirements defined by the AO, as well as acquire ancillary datasets relevant to numerous outstanding lunar science questions. In addition to the six instruments, a miniature radar, described below, was added to the payload as a technology demonstration. All data collected during the LRO mission will be delivered to the NASA's Planetary Data System within six months from the time of acquisition.

Lunar Orbiter Laser Altimeter (LOLA): LOLA will determine the global topography of the lunar surface at high resolution, measure landing site slopes, surface roughness, and search for possible polar surface ice in shadowed regions. PI, David Smith, NASA Goddard Space Flight Center, Greenbelt, MD.

LOLA Objectives:

1. Global geodetic lunar topography.
2. Characterize polar region illumination.
3. Image permanently shadowed regions.
4. Contribute to the assessment of meter-scale features to facilitate landing-site selection.
5. Identify surface polar ice, if present.

Lunar Reconnaissance Orbiter Camera (LROC): LROC will acquire targeted narrow angle images of the lunar surface capable of resolving meter-scale features to support landing site selection, as well as wide-angle images to characterize polar illumination conditions and to identify potential resources. PI, Mark Robinson, Arizona State University, Tempe, Arizona.

LROC Objectives:

1. Landing site identification and certification, with unambiguous identification of meter-scale hazards.
2. Mapping of permanent shadows and sunlit regions.
3. Meter-scale mapping of polar regions.
4. Repeat observations to enable derivation of meter-scale topography.
5. Global multispectral imaging to map ilmenite and other minerals.
6. Global black and white morphology base map.
7. Characterize regolith properties.
8. Determine recent small impactor rates by re-imaging regions photographed with the Apollo Panoramic Camera (1–2 meter m/pixel).

Lunar Exploration Neutron Detector (LEND): LEND will map the flux of neutrons from the lunar surface to search for evidence of water ice, and will provide space radiation environment measurements that may be useful for future human exploration. PI, Igor Mitrofanov, Institute for Space Research, and Federal Space Agency, Moscow.

LEND Objectives:

1. Determine hydrogen content of the subsurface at the polar regions with spatial resolution of 10 km and with sensitivity to concentration variations of 100 parts per million (ppm) at the poles.
2. Characterization of surface distribution and column density of possible near-surface water ice deposits in the Moon's polar cold traps.
3. Global mapping of Lunar neutron emissions at an altitude of 30–50 km above Moon's surface, with a spatial resolution of 5 km (pixel radius) at the spectral range of thermal energies up to 15 MeV.

Table 1 LRO products and benefits

Instrument	Example key data products	Example of exploration benefits	Example of science benefits
LOLA Lunar Orbiter Laser Altimeter	35 m polar topography at < 10 cm vertical, global topography, surface slopes and roughness	Identify safe landing sites, image shadowed regions, map potential surface ice, improve gravity field model	Global topography and gravity for interior structure and geological evolution
LROC Lunar Reconnaissance Orbiter Camera	Thousands of 50 cm/pixel images, and entire Moon at 100 m in UV, Visible. Polar illumination conditions	Surface landing hazards, locations of near constant solar illumination	Impact and volcanic processes, resource evaluation, and crustal evolution
LEND Lunar Exploration Neutron Detector	Maps of hydrogen in upper 1 m of Moon at 10 km scales, neutron albedo	Locate potential water-ice in lunar soil or concentrations of implanted hydrogen	Distribution, sources, and history of polar volatiles
DLRE Diviner Lunar Radiometer Experiment	500 m scale maps of surface temperature, albedo, rock abundance, and ice stability	Measures thermal environment in permanent shadow and permanent light ice stability depth map	Distribution, sources, and history of polar volatiles
LAMP Lyman Alpha Mapping Project	Maps of frosts and landforms in permanently shadowed regions (PSRs)	Locate potential water-ice on the surface, image shadowed areas, and map potential landing areas in PSRs	Distribution, sources, and history of polar volatiles
CRaTER Cosmic Ray Telescope for the Effects of Radiation	Lunar and deep space radiation environment and tissue equivalent plastic response to radiation	Safe, lighter weight space vehicles. Radiation environment for human presences at the Moon and journeys to Mars and beyond	Radiation boundary conditions for biological response. Map radiation reflected from lunar surface
Mini-RF Technology Demonstration	X and S-band radar imaging and interferometry	Demonstrate new lightweight SAR and communication technologies, locate potential water-ice	Source, history, deposition of polar volatiles

Diviner Lunar Radiometer Experiment (DLRE): DLRE will chart the temperature of the entire lunar surface at approximately 500 meter horizontal scales to identify cold-traps and potential ice deposits. PI, David Paige, University of California, Los Angeles.

DLRE Objectives:

1. Map global day/night surface temperature.
2. Characterize thermal environments for habitability.
3. Determine rock abundances globally and at landing sites.
4. Identify potential polar ice reservoirs.
5. Map variations in silicate mineralogy.

Lyman-Alpha Mapping Project (LAMP): LAMP will map the entire lunar surface in the far ultraviolet. LAMP will search for surface ice and frost in the polar regions and provide images of permanently shadowed regions illuminated only by starlight. PI, Alan Stern, Southwest Research Institute, Boulder, Colorado.

LAMP Objectives:

1. Identify and pinpoint surface exposed frost in Permanently Shadowed Regions (PSRs).
2. Map all permanently shadowed regions with resolutions down to 100 m.
3. Demonstrate the feasibility of natural starlight and Lyman-Alpha (α) sky-glow illumination for future lunar surface mission applications.
4. Assay the lunar atmosphere and its variability.

Cosmic Ray Telescope for the Effects of Radiation (CRaTER): CRaTER will investigate the effect of galactic cosmic rays on tissue-equivalent plastics as a constraint on models of biological response to background space radiation. PI, Harlan Spence, Boston University, Massachusetts.

CRaTER Objectives:

1. Measure and characterize the Linear Energy Transfer (LET) spectra of galactic and solar cosmic rays (particularly above 10 MeV) in the deep space radiation environment most critically important to the engineering and modeling communities to assure safe, long-term human presence in space.
2. Develop a simple, compact, and comparatively low-cost instrument, based on previously flown instruments, with a sufficiently large geometric factor to measure LET spectra and its time variation globally in the lunar orbit.
3. Investigate the effects of shielding by measuring LET spectra behind different amounts and types of areal density materials, including tissue-equivalent plastic.

Test models of radiation effects and shielding by verifying/validating model predictions of LET spectra with LRO measurements, using high-quality galactic cosmic rays (GCR) and solar energetic protons (SEP) spectra available contemporaneously with ongoing/planned NASA (ACE, STEREO, SAMPEX) and other agency spacecraft (NOAA-GOES).

An overview of the LRO products and benefits is shown in Table 1 and performance parameters in Table 2, followed by detailed instrument descriptions.

2.1 Lunar Orbiter Laser Altimeter

Topography is essential to safe lunar landings. On both a local and global scale, knowledge of the lunar surface topography is vital to landing site selection. Topography, surface slopes and surface roughness also preserve a scientific record of the evolution of the lunar surface.

The Lunar Orbiter Laser Altimeter (LOLA) has two primary objectives. First, LOLA will produce a high-resolution global topographic model and geodetic framework that will assist with precise targeting, safe landing, and surface mobility for future scientific and exploration activities. LOLA will also characterize the polar illumination environment and image the Moon's PSRs to identify possible locations of surface ice crystals in shadowed polar craters. To achieve these primary objectives, LOLA will make three measurements: 1) the distance between the surface and the spacecraft, 2) the spreading of the returned laser pulse, and 3) the transmitted and returned laser energies. LOLA is a pulse detection time-of-flight altimeter that incorporates a five-spot pattern that measures the precise distance to the lunar surface at 5 spots simultaneously, thus providing 5 profiles across the lunar surface. Each spot within the five-spot pattern has a diameter of five meters; the spots are 25 meters apart, and form a cross pattern (Fig. 1). The 5-spot pattern enables the surface slope to be derived in the along-track and across track directions; the pattern is rotated approximately 26° to provide five adjacent profiles, 10 to 12 meters apart over a 50 to 60 meter swath, with combined measurements in the along track direction every 10 to 12 meters.

Table 2 Instrument performance parameters

Instrument	Instrument classification	Characteristic range	Characteristic resolution	Spatial resolution (from 50 km)	Spatial coverage	Data rate Gbit/day
LOLA	Laser altimeter	Range window 20–70 km	10 cm vertical	Five 5 m laser spots, 25 m spacing	Polar Grid 0.001° latitude 0.04° longitude	1.4
LROC NAC	High resolution camera	Broadband centered at 550 nm	±150 nm	50 cm/pixel	Targeted >10% lunar surface 100% > 85.5° lat.	515
LROC WAC	Multi-spectral camera	315–680 nm	Spectral filters centered at 315 nm 360 nm, 415 nm, 560 nm, 600 nm, 640 nm, 680 nm	100 m/pixel vis 400 m/pixel UV	Full lunar surface at each wave-length and various lighting angles	41
LEND	Neutron detector	Thermal to 15 MeV	Four bands Thermal <0.4 eV Epithermal 0.4 eV–10 keV Fast 10 keV–1 MeV Energetic 1 MeV–15 MeV	Epithermal 10 km FWHM (see test for other bands)	Full lunar surface and deep space	0.26
DLRE	Radiometer	30 K to 400 K	5 K	400 m	Full lunar surface day/night temperatures	3.5
LAMP	UV imaging spectrograph	52 to 187 nm	3.5 nm	260 m	Full lunar surface	2
CRaTER	Primary and albedo cosmic ray sensor	LET spectra 0.2 keV/μm to 7 MeV/μm	<3%	77 km	Full lunar surface and deep space	7.8 (peak)
mini-RF	X- and S-band synthetic aperture radar	4 cm (X-band) 12 cm (S-band)	Sensitivity: −30 dB (S-band) −25 dB (X-band)	75 m/pixel, 7.5 m/pixel (zoom)	Limited during the nominal mission	7.7*

*mini-RF 7.7 Gbits for 4 min. data collection interval

LOLA will provide a 10 cm local topography in a center-of-mass coordinate system for regions displaying low slopes. The body fixed center-of-mass measurements will have a nominal accuracy of a fiducial position of ∼50 m on the surface and 1 m elevation. In addition, each 5-meter spot provides a measure of the surface roughness to ∼30 cm within the (flat) spot, derived from the spreading of the laser pulse. LOLA will also measure the relative surface reflectance within each 5-m spot at the wavelength of the laser to a 5% precision, enabling the detection of highly reflective material on the lunar surface (such as water ice crystals).

LOLA's instrument design (Fig. 2) is similar to the designs of the Mars Orbiter Laser Altimeter (Smith et al. 2001) and the Mercury Laser Altimeter (Solomon et al. 2001); however, it has five laser beams and five receiver channels. LOLA's laser transmitter consists of

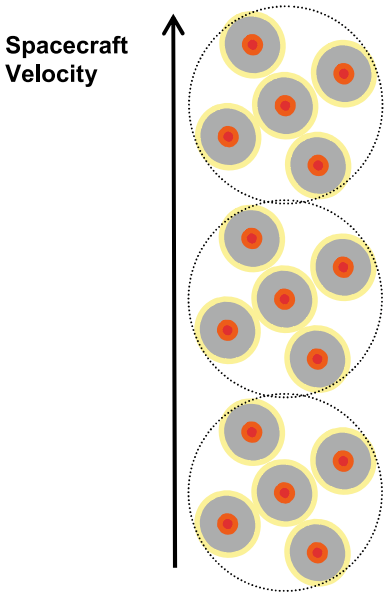

Fig. 1 Pulse detection time-of-flight altimeter 5-spot pattern. *Red* represents the laser spots on the ground while the *grey circles* represent the receiver FOV

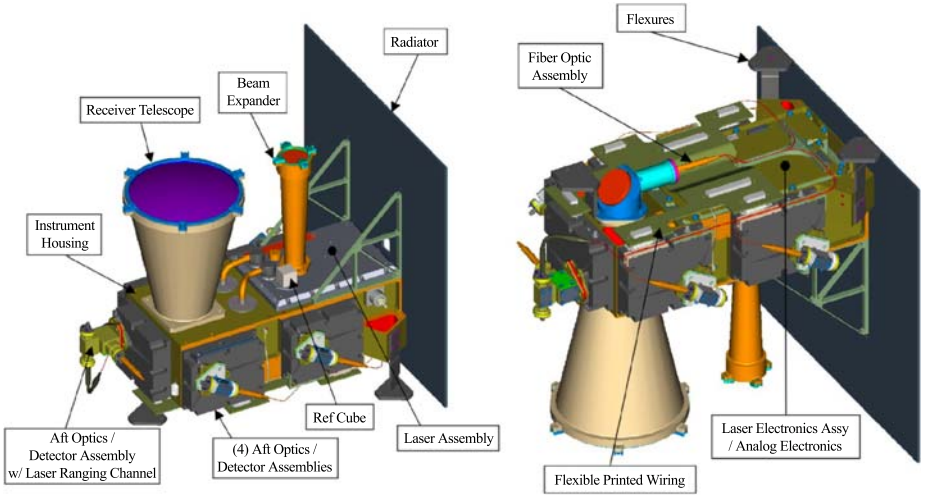

Fig. 2 LOLA instrument design

a single stage diode-pumped and Q-switched Nd:YAG laser with a 1064 nm wavelength, a 2.7 mJ pulse energy, a 6 ns pulse, a 28 Hz pulse rate, and a 100 μrad beam divergence angle. A diffractive optics element made of fused silica with an etched-in diffraction pattern is used to split the single incident laser beam into five off-pointed beams, creating the 50 meter diameter 5-spot cross-pattern on the lunar surface. The reflected signal is collected by a 14-cm diameter telescope with a 5-optical-fiber array at the focal plane. Each of the five optical fibers collects the reflected signal from one of the five laser spots on the lunar surface, and delivers it to one of the five avalanche photodiodes. The transmitted laser pulse and the

Table 3 LOLA instrument overview

Laser	
Pulse Energy	2.7 ± 0.3 mJ
Pulse width and rate	6 ns FWHM, 28 Hz
Wavelength	1064.30 ± 0.1 nm
Beam splitting	5-way, >13% total per beam
Beam divergence (per beam)	100 µrad
Beam separation	500 µrad
Receiver optics	
Receiver aperture	$A_{\text{tel}} = 0.015$ m^2 ($\phi = 0.14$ m)
Field of view	400 µrad
Optics transmission	>70%
Optical bandwidth	0.8 nm
Photodetector/preamplifier	
Detector active area	0.7 millimeter (mm)
Detector quantum efficiency	40%
Noise equivalent power	0.05 pW/Hz$^{1/2}$
Electrical bandwidth	100 MHz
Timing electronics	
Timing resolution	<0.5 ns
Clock frequency uncertainty	<1e−7
Laser pulse epoch time accuracy	<3 ms

five received laser pulses are time stamped with respect to the spacecraft mission elapsed time using a set of time-to-digital converters at <0.5 ns precision. In addition, LOLA measures the transmitted and received pulse by integrating the pulse waveforms. The on-board science algorithm, running on an embedded microprocessor, autonomously adjusts the receiver detection threshold levels and detector gain to keep the range window tracking the lunar surface returns. The key instrument parameters are listed in Table 3.

Because LOLA will make global observations, the LOLA altimetry data can be used to improve the spacecraft orbit, and our knowledge of far side lunar gravity—which is currently extremely poorly known but is required for precise landing and low-altitude navigation.

2.2 Lunar Reconnaissance Orbiter Camera

The LROC is designed to address two of the prime LRO measurement requirements: 1) Assess meter and smaller-scale features to *facilitate safety analysis for potential lunar landing sites* anywhere on the Moon; and 2) Acquire multi-temporal synoptic imaging of the poles every orbit to *characterize the polar illumination environment* (on a 100 m scale), identifying regions of permanent shadow and permanent or near-permanent illumination over a full lunar year. The LROC consists of two narrow-angle cameras (NACs) (see Fig. 3) to provide 0.5 m scale panchromatic images over a 5 km swath, a wide-angle camera component (WAC) (see Fig. 4) to provide images at a scale of 100 m in seven color bands over a 100 km swath in black and white mode and 60 km in color mode, and a common Sequence and Compressor System (SCS).

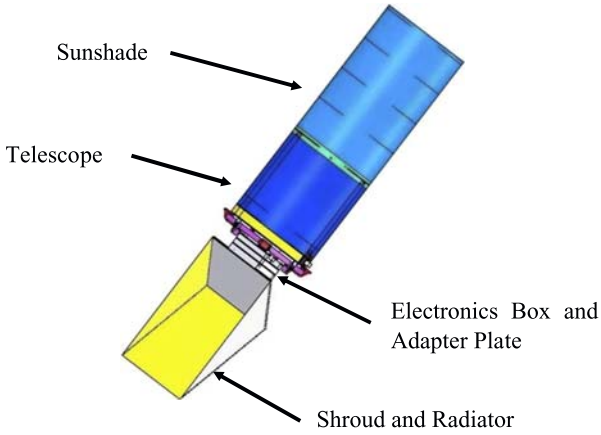

Fig. 3 LROC narrow angle camera, 70 cm length by 24 cm diameter

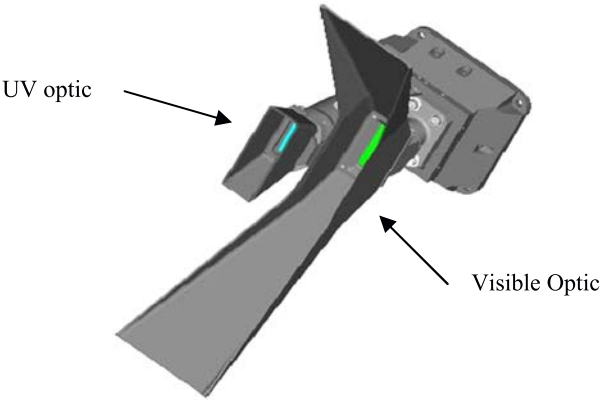

Fig. 4 LROC wide angle camera, 14.5 cm by 9.2 cm by 7.6 cm

In addition to acquiring the two LRO prime measurement sets, LROC will return six other high-value datasets that support LRO goals, the LPRP, and basic lunar science. These additional datasets include:

- Meter-scale imaging of regions of permanent or near-permanent illumination.
- Multiple co-registered observations of portions of potential landing sites and elsewhere for derivation of high-resolution topography through stereogrammetric and photometric stereo analyses.
- A global multispectral map in 7 wavelengths (315–680 nm) useful for mapping potential lunar resources, in particular ilmenite.
- A global 100-m/pixel basemap with incidence angles (60–80°) favorable for morphologic interpretations.
- Sub-meter imaging of a variety of geologic units to characterize physical properties, variability of the regolith, and key science questions.
- Meter-scale coverage overlapping with Apollo era Panoramic images (1–2 m/pixel) to document the number of small impacts since 1971–1972, to ascertain hazards for future surface operations and interplanetary travel.

LROC has high heritage from the Mars Reconnaissance Orbiter (MRO) Context Camera (CTX) and Mars Color Imager (MARCI) instruments (Malin et al. 2001), with modifications needed to meet the primary measurement requirements. Each NAC has a 700 mm-focal-length, Ritchey-Chretien telescope that images onto a 5000-pixel CCD line-array, providing a cross-track field-of-view (FOV) of 2.86°. The NAC readout noise is better than 100 e^-, and the data are sampled at 12 bits, then compressed to 8-bit, square root encoded-values prior to downlink. The NAC internal buffer holds 256 MB of uncompressed data, enough for a full-swath image 25 km long or a 2×2 binned image 100 km long. The WAC electronics are a copy of those flown on cameras on Mars Climate Orbiter, Mars Polar Lander, Mars Odyssey, and Mars Reconnaissance Orbiter and planned for flight on Mars Phoenix Lander. The WAC has two short-focal-length lenses imaging onto the same 1000×1000 pixel, electronically shuttered CCD area-array, one imaging in the visible/near Infrared (EFL = 6.0 mm), and the other in the UV (EFL = 4.5 mm). The optical systems have a cross-track FOV of 90° and 60° respectively. From the nominal 50 km orbit, the WAC will provide a nadir, ground sample distance of 100 m/pixel in the visible, and a swath width of ∼100 km. The seven-band color capability of the WAC is provided by a color filter array mounted directly over the detector, providing different sections of the CCD with different filters acquiring data in the seven channels in a "pushframe" mode. Continuous coverage in any one color is provided by repeated imaging at a rate such that each of the narrow framelets of each color band overlap. The LROC team will reconstruct WAC color for small areas of the Moon to demonstrate the validity of the calibration and the utility of the dataset. The WAC has a readout noise of less than 40 e^-, and, as with the NAC, pixel values are digitized to 12-bits and are subsequently converted to 8-bit values.

The NACs and WAC interface with the SCS, the third element of the LROC. As the name implies, the SCS commands individual image acquisition by the NACs and WAC from a stored sequence, and applies lossless compression to the NAC and WAC data as they are read out and passed to the spacecraft data system. The SCS provides a single command and data interface between the LROC and the LRO spacecraft data system. The SCS design is derived from the MARCI interface adapter, a digital converter unit that links the MARCI electronics on MRO to that spacecraft's data system.

Each NAC has an estimated mass of 5.4 kg, the WAC is 0.6 kg, and the SCS is 0.6 kg. Other components (radiator, mounting plate etc.) lead to a total LROC mass of 16 kg. Each NAC will use 10 W during image acquisition or readout, 6 W at all other times; the WAC will use 4 W (continuous), and the SCS will use 6 W (continuous), for a total LROC power dissipation of 30 W peak, 22 W average.

The LROC Science Operations Center (SOC) will be located at Arizona State University where all uplink and downlink activities will take place. The SOC is scaled assuming a 300 Gbit/day downlink with lossless compression, producing a total of 20 TeraBytes (TB) of uncompressed raw data over the nominal mission. Production of higher-level data products will produce a total of 70 TB for Planetary Data System archiving. To reduce schedule risk LROC is leveraging existing software, with targeting and sequencing software derived from Mars Global Surveyor-MOC and MRO-CTX, and automated downlink processing derived from MRO-HiRISE (High Resolution Imaging Science Experiment) procedures with the USGS Integrated Software for Imagers and Spectrometers (ISIS) package for radiometric and geometric processing (Eliason et al. 1999). LROC data will be disseminated via web interface in raw, calibrated, and mosaicked versions.

2.3 Lunar Exploration Neutron Detector

Neutrons from the Moon are produced in the subsurface layer of 1–2 m of regolith due to bombardment by galactic cosmic rays (GCR). These secondary neutrons diffuse in the subsurface material and interact with soil nuclei with the emission of nuclear gamma-rays. All celestial bodies without a thick atmosphere, like the Moon, Mars, Mercury, and asteroids, produce secondary neutron emission. Neutrons from these celestial bodies have a range of energies. Original high energy neutrons produced by GCR have energies about tens of MeV. In each collision with nuclei, neutrons lose some fraction of their energy, and many of them are moderated down to the thermal energy of the regolith. Other neutrons escape before being thermalized and have some intermediate energy between tens of MeV and the regolith thermal energy.

The detection of lunar gamma-rays was pioneered in April 1966 by Alexandr Vinogradov, Yury Surkov and colleagues with the Soviet lunar orbiter, Luna-10 (Vinogradov et al. 1966). The first measurements of lunar gamma-rays were made by James Arnold, Albert Metzger, Jacob Trombka and colleagues in 1971 and 1972, from the orbiting Command and Service modules of Apollo 15 and 16 (Metzger et al. 1973). The first global mapping of neutron emissions from the Moon was performed in 1998–1999 by William Feldman and colleagues using the omni-directional Neutron Spectrometer on NASA's Lunar Prospector (Feldman et al. 1998). The data yielded by these missions shows that emission of epithermal neutrons decreases in the lunar polar regions in comparison with lower latitudes.

It is known that higher hydrogen content in the soil leads to faster moderation of neutrons, and therefore decreases the fraction of leaking epithermal neutrons and correspondingly increases the fraction of leaking thermal neutrons (Feldman et al. 1998). The presence of 100 ppm of hydrogen in the lunar regolith would lead to a decrease of epithermal neutron flux by about 5% in comparison to the absence of hydrogen. Therefore, mapping the epithermal neutron emissions of the Moon is the most powerful method to determine the distribution of hydrogen in the shallow subsurface of the Moon (up to 1–2 meters). Evidence for lunar polar depression of epithermal neutron flux from the Lunar Prospector has two alternative interpretations: the first (Feldman et al. 2000) attributes depression of epithermal neutrons to water-ice deposits at in permanently shadowed craters, the other interpretation explains polar neutron depression as the enhancement of hydrogen implanted from solar wind due to a slow diffusion process at low polar temperatures (Vondrak 1988).

The Lunar Exploration Neutron Detector's (LEND's) most important attribute is that it is capable of providing high spatial resolution mapping of epithermal neutrons with collimated epithermal neutron detectors (see detectors CSETN 1–4 in Fig. 5). LEND is able to detect a hydrogen-rich spot at one of the Lunar poles with as little as 100 ppm of hydrogen and a spatial resolution of 10 km (pixel diameter), and to produce global measurements of the hydrogen content with a resolution of 5–20 km. If the hydrogen is associated with water, a detection limit of 100 ppm hydrogen corresponds to $\sim 0.1\%$ weight water ice in the regolith. High energy neutron data from another LEND sensor (SHEN in Fig. 5) could help to distinguish between areas in which hydrogen was implanted by solar wind and potential water ice deposits. However, the most conclusive results from the reconnaissance of lunar water/hydrogen resources would come from the joint analysis of all mapping science instruments onboard LRO: DLRE, LAMP, LEND, LOLA and LROC.

Neutron radiation from the regolith could have as large an impact on astronaut safety as energetic charged particles from GCR and Solar Particle Events (SPEs). The main radiation effect from GCR and SPE protons is from Coulomb interactions. CRaTER will measure these particles on LRO. Neutrons interact with matter by direct collisions with nuclei and

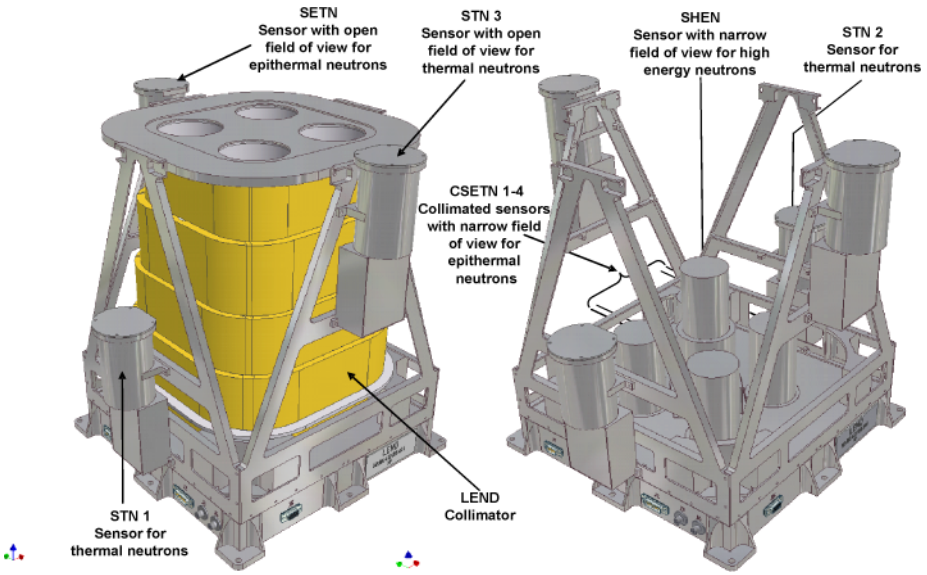

Fig. 5 LEND Design Concept with four collimated sensors of epithermal neutrons CSETN 1–4, one sensor with narrow FOV for high energy neutrons SHEN and four sensors of thermal STN 1–3 and epithermal SETN neutrons with open fields of view. Left view is LEND with the collimator and right view is LEND without the collimator

creation of spallation products and radioactive isotopes. The radiation damage to human tissue could be quite different in these two cases, although it is currently unknown which is worse. LEND will have a full set of sensors for thermal (STN 1–3), epithermal (SETN) and high energy neutrons (SHEN) to provide data for neutron components of radiation environment in the broad range of more than 9 decades of energy.

The Russian-made, Russian-supplied instrument Lunar Exploration Neutron Detector (LEND) uses a design based on the Russian High Energy Neutron Detector (HEND), which continues to perform well in its fifth year of science measurements onboard NASA's Mars Odyssey (Mitrofanov et al. 2002). LEND and HEND have similar types of neutron sensors, and HEND's observations on Martian water resources have proven the sensitivity this technique for planetary exploration.

LEND's primary sensor type is the ^{3}He counter, used for LEND detectors CSETN 1–4, STN 1–3, and SETN. The ^{3}He counter produces an electrical pulse proportional to the number of ions formed. The Cd shield around CSETN 1–4 and SETN absorbs all neutrons with energies below ∼0.4 eV, which exclude all thermal neutrons from detection. The major difference between LEND and HEND, is the collimation of neutron flux before detection. Collimating modules around the ^{3}He counters of CSETN 1–4 effectively absorb neutrons that have large angles with respect to the normal on the Moon's surface (Fig. 5), leading to spatial resolution of 10 km full width at half maximum signal from the nominal 50 km orbit. This is the first time this method of "neutronography" will be used to map another planet with high spatial resolution.

A numerical simulation of LEND performance showed that the instrument, with the optimal shaping of the collimators of sensors CSETN 1–4, may provide a detection limit (3 sigma) of Hydrogen of about 82 ppm for a polar spot with a diameter of 10 km (FWHM),

Table 4 Estimated detection limit (3 sigma in ppm) of hydrogen for different spots in the polar region of the Moon

Latitude and distance from Poles	Size of spot (radius, km)		
	5	6	10
89° (30 km)	82.5	56.0	28.4
87° (90 km)	278.8	164.2	62.8
85° (150 km)	726.5	398.6	144.6

given a baseline 1 year mapping mission from a 50 km polar orbit. This detection sensitivity increases for larger spots, and decreases for locations more distant from the pole (Table 4).

The second type of LEND neutron detector is the stilbene scintillator, which produces a flash of light each time a high energy neutron in the range 0.3–15.0 MeV collides with a hydrogen nucleus and creates a recoil proton. Special electronics distinguish protons from electrons, and an active anti-coincidence shield eliminates external charged particles.

LEND's set of 8 different detectors with ^{3}He counters (4 of which have collimators) and one stilbene scintillator will provide the observational data necessary for global mapping of the hydrogen content on the lunar surface, with a spatial resolution of 5 km radius at the poles. LEND measurements will also allow for the characterization of the neutron component of the lunar radiation environment.

2.4 Diviner Lunar Radiometer Experiment

The Diviner Lunar Radiometer Experiment (DLRE) will provide a complete set of precise radiometric lunar surface temperature measurements over the full 40–400 K anticipated range. Over the course of the LRO mission, Diviner will acquire a dataset of fundamental importance to future human exploration. Data obtained by Diviner may be used to assess day and night surface and subsurface thermal conditions, or to determine rock abundances at future landing sites. Diviner will also identify and characterize permanently shadowed cold-traps that may contain near-surface water ice resources.

The nine-channel Diviner visible and infrared radiometer closely follows the design of the 2005 Mars Reconnaissance Orbiter (MRO) Mars Climate Sounder (MCS) (McCleese et al. 2007) (Fig. 6). The MCS employs precise multichannel filter radiometry to measure vertical temperature profiles, dust and water vapor in the Martian atmosphere, as well as the Martian surface temperature. The LRO DLRE will use the same general-purpose filter radiometer capabilities to measure lunar surface temperatures, however, a different set of spectral filters will be used and the signal sampling rate will be increased.

Table 5 shows the spectral response of the nine Diviner channels. Figure 7 shows the spectral response of Diviner's seven infrared channels compared to the thermal emission spectra of representative blackbodies. Figure 8 shows the results of model calculations of diurnal temperature variations on the moon. Diviner will have a sufficiently low minimum detectable temperature to map lunar surface temperatures over the full anticipated range. With these measurements, Diviner will be capable of:

- Mapping global day/night surface temperatures and characterizing lunar environments for habitability.
- Determining fine-component thermal inertias and rock abundances by mapping nighttime surface temperatures in multiple spectral channels.
- Identifying polar cold traps in permanently shadowed regions and potential water ice resources.

Fig. 6 The MRO MCS flight model during thermal vacuum testing at JPL

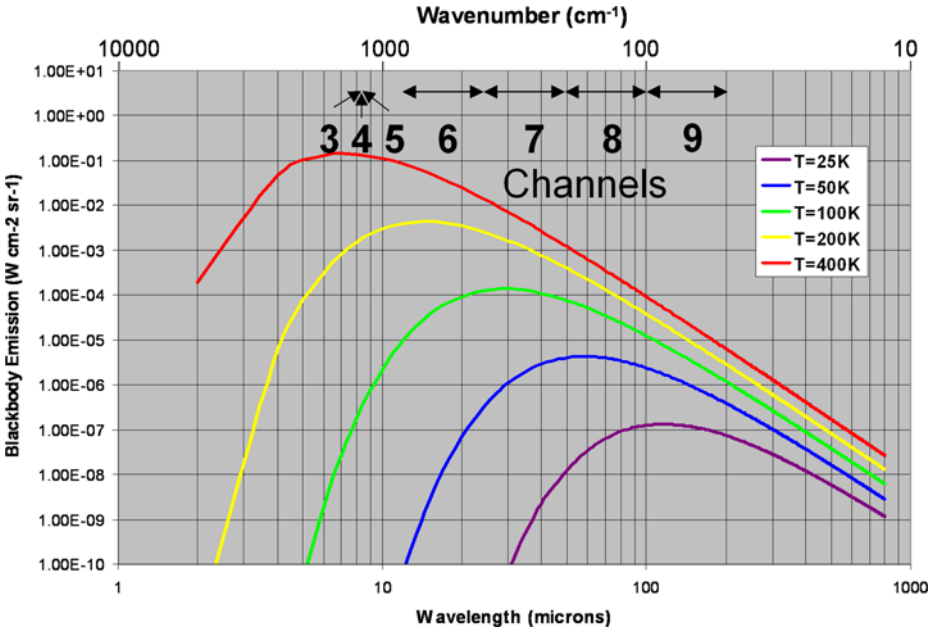

Fig. 7 The locations of Diviner's seven infrared channels and the spectral emission of blackbodies at 25 to 400 K

- Mapping variations in silicate mineralogy by determining the wavelength of the Christiansen spectral emission feature near 8 microns.

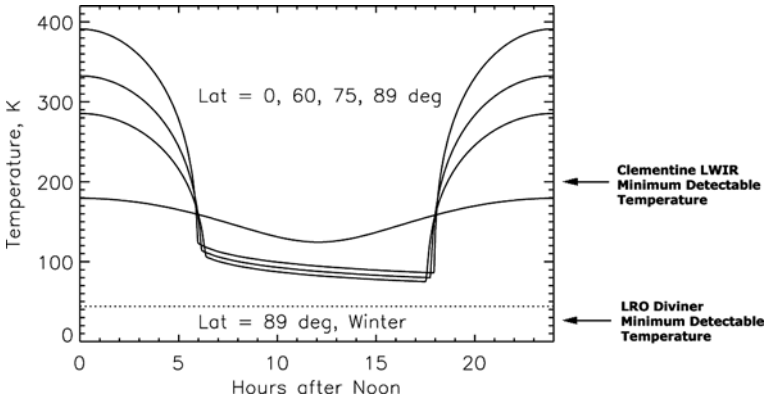

Fig. 8 Model calculated diurnal lunar surface temperature variations over a complete diurnal cycle for horizontal surfaces at latitudes (from top to bottom) of 0°, 60°, 75°, and 89° (summer) or 90° (winter)

Table 5 DLRE's nine spectral channels

Telescope	Channel number	Minimum wavelength (microns)	Maximum wavelength (microns)	Purpose	Minimum detectable signal
A	1	0.3	3	Solar reflectance in permanently shadowed regions	40 K[1]
A	2	0.3	3	Solar reflectance in sunlit regions	55 K[1]
A	3	7.88	8.13	Thermal emission near Christiansen feature	160 K
A	4	8.13	8.38	Thermal emission near Christiansen feature	160 K
A	5	8.38	8.63	Thermal emission near Christiansen feature	160 K
A	6	12.5	25	Thermal mapping	75 K
B	7	25	50	Thermal mapping	45 K
B	8	50	100	Thermal mapping	32 K
B	9	100	200	Thermal mapping	30 K

[1]Intensity of reflected radiation from an isotropic reflector with broadband solar albedo of 0.1 in thermal equilibrium at the quoted temperature.

Diviner will operate continuously in nadir push-broom mapping mode using 21 detectors cross-track for each of its nine spectral channels. The FOV of each detector is 3.6 mrad cross track, yielding a resolution of 180 m on the lunar surface at an orbital altitude of 50 km. To facilitate spatial registration of Diviner's surface footprints in multiple spectral bands, and to reduce along-track smear, Diviner's integration period will be 0.128 seconds. Diviner's mapped data products will generally be at a resolution of ∼500 m/pixel to increase Signal to Noise Ratio (SNR), and to allow for anticipated errors in the reconstruction of the position and pointing of the LRO spacecraft.

It is likely that Diviner's most important measurements will be those taken in the lunar polar regions, where it has been predicted that temperatures in the permanently shadowed regions may be cold enough (40–110 K) to trap water ice for billions of years. Diviner has the necessary sensitivity and coverage to accurately map surface temperatures in the PSRs down to approximately 30 K. Diviner's measurements may be used to determine favorable

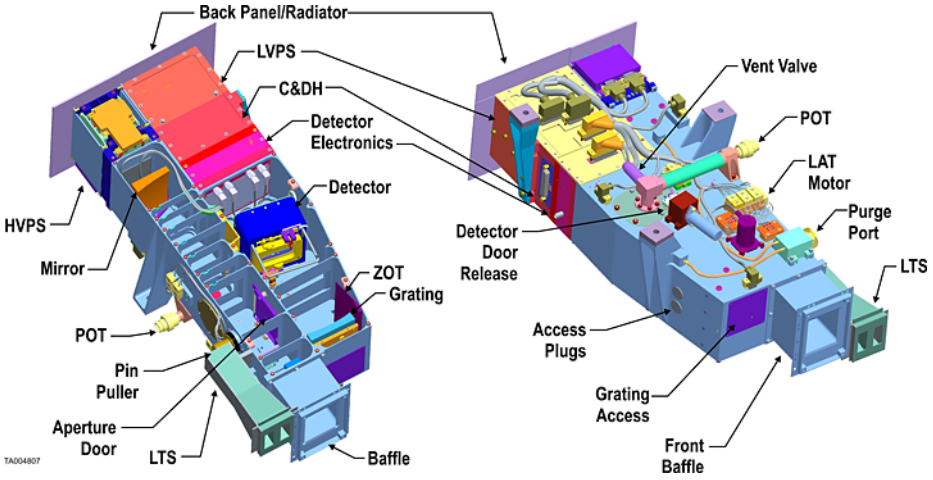

Fig. 9 LAMP design as seen from above (left) and below (right); the forward baffle discussed in the text is not shown here

landing sites, based on surface and subsurface thermal stability of water ice deposits. In conjunction with the other instruments on LRO, Diviner will produce a clearer picture of the distribution and properties of the Moon's polar ice deposits.

2.5 The Lyman-Alpha Mapping Project

The objectives of the Lyman-Alpha Mapping Project (LAMP) investigation are to:

- Search for exposed water ice near the lunar poles and in PSRs using reflected Lyman-Alpha (α) sky-glow and far-ultraviolet starlight.
- Obtain landform maps in the PSR regions and serve as a pathfinder for a lunar natural light night vision system.
- Obtain data on the tenuous lunar atmosphere.

The LAMP instrument (shown in Fig. 9) is a near-clone of the sensitive (∼1 Rayleigh level), lightweight (∼4 kg), low-power (∼4 W) ALICE imaging UltraViolet Spectrometer (UVS) selected and delivered for flight on both the European Space Agency/NASA Rosetta comet orbiter (Slater et al. 2001) and NASA New Horizons missions (Stern et al. 2005).

The presence of an excess hydrogen (H) signature, as detected by neutron spectroscopy, cannot guarantee the hydrogen is in the form of water without other supporting measurements. LAMP provides LRO with the unique capability of being able to *spectrally fingerprint* exposed H_2O frost in the lunar polar regions. This will be accomplished using observations illuminated purely by Lyman-α sky-glow and broadband far ultra-violet (FUV) starlight. The lifetime of exposed water frost in polar cold traps is predicted to be short, owing to regolith gardening and sputtering processes. However, even if this is true, thin surface deposits of recently deposited frost must exist in an equilibrium set by the balance between source and loss rates to the pole; their discovery would be a major find for LRO. Water ice has a diagnostic spectral reflectance signature at 120–180 nm, as evidenced by ultraviolet spectra obtained in the laboratory as well as on icy surfaces in the solar system. Owing to this signature, FUV spectroscopy provides a way to directly fingerprint H_2O-frost exposed on the lunar surface, even at the relatively small (∼4%) mixing ratios predicted by volatile

transport models and the 1.5% level. To make these detections LAMP will obtain spectral maps across the lunar surface, and retrieve H_2O frost abundances (or strong upper limits) by rationing PSR spectra to those of waterless ("dry") regions away from the PSRs. Sky illumination brightness variations can be accounted for using public-archive data available from various instruments now in space (e.g., SWAN on SOHO).

The same data collected to achieve LAMP's water frost mapping objective also satisfies the objective of creating landform maps of the PSRs. Using only FUV starlight and Lyman-α sky-glow, LAMP is capable of mapping even the darkest PSRs (where no reflected sunshine or Earthshine is available—e.g. Shackleton Crater) with 100 m class spatial resolution. Other LRO instruments are capable of mapping the regions illuminated by scattered sunlight, where LAMP's Signal to Noise Ratio (SNR) will be higher.

LAMP data will also be used to compile the first FUV albedo maps of the entire Moon assembled over the course of the baseline mission.

In addition, LAMP will serve as the first demonstration that the same technology used by military night vision equipment, using UV starlight and Lyman-α sky-glow as its light source, can be applied to space exploration. LAMP will prove the technique's feasibility for future use, e.g. ground based lunar polar/night vision systems. Such a natural light vision system could provide vision capability for future rover and human exploration at night, or in PSRs, without any of the power demands associated with operating artificial lighting at night or in polar regions.

Finally, LAMP will provide a new generation of UV spectral exploration of the lunar atmosphere. The lunar atmosphere, with a total mass of order 40 tons, is one of several Surface Boundary Exosphere (SBE) atmospheres in the solar system (Stern 1999) (other SBEs of note include the atmospheres of Mercury, Europa, and Ganymede). Species detected in (or from) the lunar atmosphere include Ar, Na, K, Al, Si, and O. Of these, Ar, detected by the Apollo 17 LACE mass spectrometer, appears to be an internal release product generated by K decay; Na and K are sputter- or meteoritic-vaporization products detected as atomic neutrals; O, Si, and Al are probably similarly derived but have to date only been detected as ions by instruments on the AMPTE and ISEE missions downwind of the Moon. LAMP's wavelength range allows it to follow already-detected atmospheric Ar (104.8, 106.6 nm) over repeated lunations to better characterize the sources and sinks. Argon is particularly interesting, since it dominantly comes from the lunar interior and may be tied to specific release sites that could be of interest for future landing site selection. Because the atmospheric H distribution is a tracer of water vapor transport to the lunar poles, maps of the time-averaged H distribution as a function of latitude are expected to reveal a deficit ("polar holes") at high latitude which could constrain the rate of water transport to the polar regions.

The LAMP instrument is essentially a copy of the Pluto ALICE (P-ALICE) instrument design (Slater et al. 2001; Stern et al. 2005), with only very minor changes. In this section we provide a brief description of the instrument. The primary differences between LAMP and Pluto-Alice are in the area of spacecraft accommodation—i.e., changes to mounting feet, the addition of cooling radiators, the addition of a forward light baffle to block light scattered from other LRO instruments near LAMP, and the addition of a terminator sensor to gate the instrument on and off.

LAMP is comprised of a telescope and Rowland-circle spectrograph. LAMP has a single 40×40 mm^2 entrance aperture that feeds light to the telescope section of the instrument. Entering light is collected and focused by an $f/3$ off-axis paraboloidal (OAP) primary mirror at the back end of the telescope section onto the instrument's entrance slit. After passing through the entrance slit, the light falls onto a toroidal holographic diffraction grating, which disperses the light onto a double-delay line (DDL) microchannel plate (MCP) detector. The

2-D (1024×32)-pixel format detector is coated by a CsI solar-blind photocathode and has a cylindrically-curved MCP-stack that matches the Rowland-circle. LAMP is controlled by an Intel 8052 compatible microcontroller, and utilizes lightweight, compact, surface mount electronics to support the science detector, as well as the instrument support and interface electronics.

The OAP mirror and diffraction grating are constructed from monolithic pieces of aluminum, coated with electroless nickel and polished using low-scatter polishing techniques. The aluminum optics, in conjunction with the aluminum housing, form an a thermal optical design. Both the OAP mirror and the grating are overcoated with sputtered MgF_2 for optimum reflectivity within the FUV spectral passband. Additional control of internal stray light is achieved using internal baffle vanes within both the telescope and spectrograph sections of the housing, a holographic diffraction grating that has low scatter and near-zero line ghost problems, and an internal housing with alodyned aluminum surfaces. In addition, the zero order baffle is treated with a nickel–phosphorus (Ni–P) black coating with very low surface reflectance at EUV/FUV wavelengths.

The 2-D imaging photon-counting detector located in the spectrograph section of the instrument utilizes an MCP Z-stack that feeds the DDL readout array. The input surface of the Z-stack is coated with an opaque photocathode of CsI[24]. The detector tube body is a custom design made of a lightweight brazed alumina-Kovar structure that is welded to a housing that supports the DDL anode array.

To capture the entire 52–187 nm passband and 6° spatial FOV, the size of the detector's active area is 35 mm (in the dispersion direction) by 20 mm (in the spatial dimension), with a pixel format of 1024×32 pixels. The 6° slit-height is imaged onto the central 22 of the detector's 32 spatial channels; the remaining spatial channels are used for dark count monitoring. Our pixel format allows Nyquist sampling with a spectral resolution of 3.6 Å, and an angular resolution of ∼0.6°.

The LAMP instrument support electronics are largely single-string, but include redundant features in certain high-value areas (e.g., the power supplies). The LAMP electronics include two low-voltage power supplies, actuator electronics, the Command & Data Handling (C&DH) electronics, the optics decontamination heater system, and two detector high-voltage power supplies. All of these elements are controlled by a radiation-hardened version of the Intel 8052 microprocessor with 32 kB of fuse programmable PROM, 128 kB of EEPROM, 32 kB of SRAM, and 128 kB of acquisition memory. The C&DH electronics are contained on four circuit boards located just behind the detector electronics.

2.6 Cosmic Ray Telescope for the Effects of Radiation

The Cosmic Ray Telescope for the Effects of Radiation (CRaTER) is designed to answer key questions to enable future human exploration of the Solar System, and to address one of the prime objectives of LRO. Specifically, CRaTER addresses an objective required by NASA's Exploration Initiative to safely return humans to the Moon; CRaTER is designed to achieve *characterization of the global lunar radiation environment and its biological impacts and potential mitigation, as well as investigation of shielding capabilities and validation of other deep space radiation mitigation strategies involving materials.* CRaTER will fill knowledge gaps regarding radiation effects, provide fundamental progress in knowledge of the Moon's radiation environment, and provide specific path-finding benefits for future planned human exploration. CRaTER's primary measurement goal is to measure directly the linear energy transfer (LET) spectra caused by space radiation penetrating shielding material. Such LET

spectra are a missing link, currently derived by models which require experimental measurements to provide ground truth. CRaTER will provide this essential information about the lunar radiation environment.

LET is defined as the mean energy absorbed locally, per unit path length, when an energetic particle traverses material. A LET spectrometer measures the amount of energy deposited in a detector of known thickness and material property when an energetic particle passes through it, usually without stopping. LET measurements behind various thicknesses and types of material are of great importance to spacecraft engineers and radiation health specialists. Such measurements are especially important to modelers who study the impacts of the penetrating radiation; LET is one of the most important inputs for predictive models of human health risks and radiation effects in electronic devices. While LET spectrometers do not necessarily resolve particle mass, LET measurements do include all the species, with the possible exception of neutrons, that are relevant to the energy deposited behind a known amount of spacecraft shielding. A LET spectrometer essentially provides the key direct measurement needed to bridge the gap between well measured cosmic ray intensities (that will be available from other spacecraft) and specific energy deposition behind shielding materials, exploration-enabling knowledge vital to the safety of humans working in the harsh space radiation environment. Accordingly, CRaTER is designed to measure this important quantity and thereby provide critical closure between measurements, theory, and modeling.

CRaTER will measure LET spectra produced by incident galactic cosmic rays (GCRs) and solar energetic protons (SEPs). GCRs and SEPs with energies >10 MeV have sufficient energy to penetrate even moderate shielding. When they interact with matter, they leave behind energy, damaging the human tissue and electronic parts they pass through. GCRs and SEPs possess both short and long timescale variations (see Fig. 10), some of which are predictable and others that are not presently predictable. GCRs are a slowly-varying and uniform source of cosmic radiation that bathes the solar system. SEPs are episodic and rare, but come in extreme bursts associated with intense solar magnetic activity. Both GCRs and SEPs pose serious risks to humans venturing above the relative safety of low-Earth orbit and the Earth's powerful magnetic shield; areas including the Moon and the interplanetary space between Earth and Mars may be dangerous to humans.

In order to achieve the LRO radiation mission requirement, CRaTER is designed to return the following required data products:

- Measure and characterize that aspect of the deep space radiation environment, LET spectra of galactic and solar cosmic rays (particularly above 10 MeV), most critically important to the engineering and modeling communities to assure safe, long-term, human presence in space.
- Investigate the effects of shielding by measuring LET spectra behind different amounts and types of areal density, including tissue-equivalent plastic.

The CRaTER measurement concept is shown in the see-thru telescope drawing below (Fig. 11). The investigation hardware consists of a single, integrated telescope and electronics box with straightforward electronic and mechanical interfaces to the spacecraft. The zenith–nadir viewing telescope employs a stack of three pairs of detectors embedded within aluminum structure and tissue-equivalent plastic (TEP) to establish the LET spectra of cosmic radiation relevant for human health and electronics part concerns.

Primary GCRs and SEPs enter the telescope through the zenith, deep-space entrance, depositing energy in the telescope stack through ionizing radiation and producing secondary particles through nuclear interactions. The primary and secondary particles interact with one or more of the six detectors through the stack: the thin (thick) detectors are optimized for

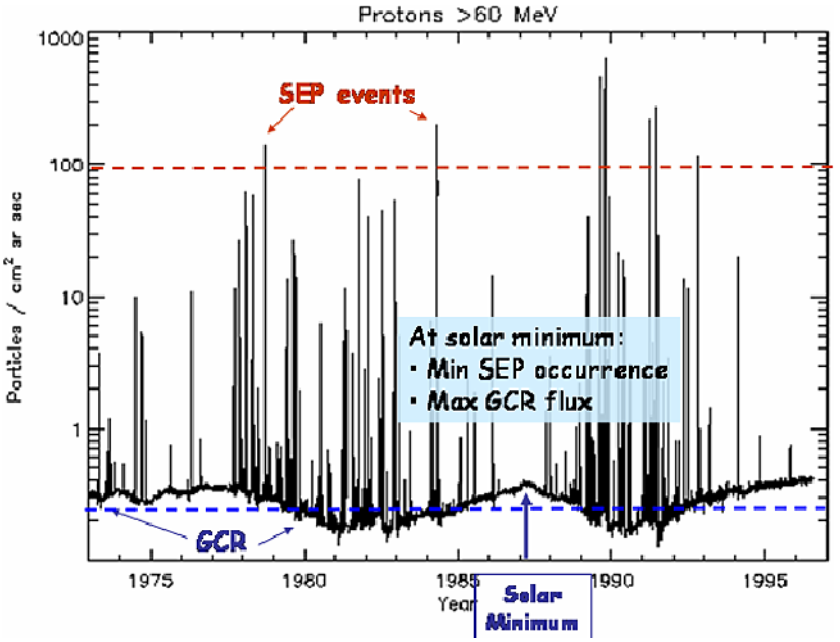

Fig. 10 GCR/SEP timescale variations

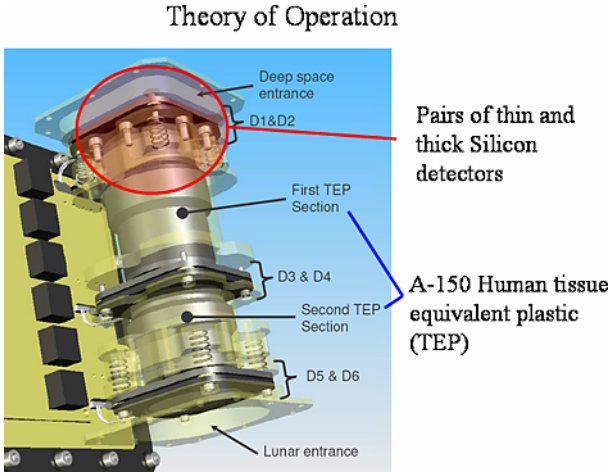

Fig. 11 CRaTER measurement concept

high (low) LET interactions. Events with sufficient energy deposition in a detector cross a trigger threshold. Digital logic then compares multi-detection coincidences with predefined event masks to identify desirable events. Pulse height analysis is performed on every detector to measure LET at each point in the stack.

The measurement team will use observations taken during the mission to construct LET spectra behind the different amounts of material, including TEP, as a function of particle environment (GCR vs. SEP; foreshock vs. magnetotail vs. solar wind; etc.). The team will also test models of radiation effects and shielding by verifying/validating deterministic models.

Model predictions of energy transport of incident GCR and SEP spectra (available contemporaneously on other missions) through the CRaTER instrument will be compared to the measured LET spectra. Thus, CRaTER will provide not only direct measurements of LET in the lunar environment, but will also better constrain radiation effects models that are being used to assess the effects of other radiation environments, including in interplanetary space and at Mars.

2.7 Robustness and Resiliency of the LRO Instrument Suite

Each of the six selected LRO instruments has strong individual capabilities and assets, and was chosen for LRO based on the delivery of a specific set of data products. In concert, the LRO instrument suite addresses LRO measurement goals in a robust and resilient manner, by using several complementary methods that reinforce the discoveries of any individual instrument. Table 6 summarizes the LRO measurement objectives and discusses the instrument(s) with data products that aim to address them.

Table 6 All LRO measurement objectives are met by several complementary data products from different instruments

LRO measurement objective	LRO instrument	Data product
The LRO shall characterize the deep space radiation environment at energies in excess of 10 MeV in lunar orbit, including neutron albedo	LEND	Radiation Data Product for global distribution of neutrons at Moon's orbit with spatial resolution of 50 km at different energy ranges from thermal energy up to >15 MeV separately for periods of quiet Sun and for periods of Solar Particle Events
	CRaTER	Provide Linear Energy Transfer (LET) spectra of cosmic rays (particularly above 10 MeV), most critically important to the engineering and modeling communities to assure safe, long-term, human presence in space
The LRO shall measure the deposition of deep space radiation on human equivalent tissue while in the lunar orbit environment	CRaTER	Provide LET spectra behind different amounts and types of areal density, including tissue-equivalent plastic
The LRO shall measure lunar terrain altitude to a resolution of 10 cm and an accuracy of 1 m for an average grid density of approximately 0.001 degrees latitude by 0.04 degrees longitude	LOLA	Provide a global digital elevation model of the Moon with 10 cm vertical resolution, 1 m vertical accuracy and 50–100 m horizontal resolution with 1 km average cross track sampling at the equator
The LRO shall determine the horizontal position of altitude measurements to an accuracy of 100 m	LOLA	Provide global topography of the Moon with 10 cm vertical resolution, 1 m vertical accuracy and 50–100 m horizontal resolution with 1 km average cross track sampling at the equator
	LROC	For targets of high interest, collect multi-look NAC data reducible to 2 m scale Digital Elevation Models for 25 km^2 areas
	LROC	Acquire 100 m/pixel global stereo imaging *reducible* to 1 km/pixel global topography in EDR format

Table 6 (*Continued*)

LRO measurement objective	LRO instrument	Data product
The LRO shall obtain temperature mapping from 40–300 K in the Moon's polar regions to better than 500 m spatial resolution and 5 K precision for a full diurnal cycle	DLRE	Temperature maps at better than 500 m spatial resolution from 40–300 K over an entire diurnal cycle to enable the detection and characterization of cold traps in polar shadowed regions
The LRO shall obtain imaging of lunar surfaces in permanently shadowed regions at better than 100 m spatial resolution	LOLA	Provide global topography with 10 cm vertical resolution, 1 m vertical accuracy and 50–100 m horizontal resolution with 1 km average cross track sampling at the equator
	LAMP	Albedo maps of all permanently shadowed regions with resolutions up to 100 m
The LRO shall identify putative deposits of water-ice in the Moon's polar cold traps at a spatial resolution of better than 500 m on the surface and 10 km subsurface (up to 2 m deep)	LOLA	Provide Reflectance data from the permanently shadowed regions to identify surface ice signatures at a limit of 4% ice surface coverage by area
	LEND	Develop maps of putative water-ice column density on polar regions of the moon with spatial resolution of 10 km
	LAMP	Develop water-frost concentration maps of the lunar polar regions. Mapping resolutions as good as 3 km for frost abundances down to 1.5%
The LRO shall assess meter-scale features of the lunar surface to enable safety analysis for potential lunar landing sites over targeted areas of 100 km^2	LROC	Provide up to 50 mosaics of selected potential landing sites with one meter scale resolution
	LROC	Provide crater size density and size distribution maps of up to 10 potential landing sites (100 km^2/site)
	DLRE	Provide rock ($\geq$0.5 m diam.) abundance percentages for up to 50 selected potential landing sites by measuring the ratio of high thermal to low thermal inertia material
	LOLA	Provide topography, surface slopes, and surface roughness at 25-m spacing over a 70 m wide FOV swath at up to 50 selected potential landing sites
The LRO shall characterize the Moon's polar region illumination environment to a 100 m spatial resolution and 5 Earth hour average temporal resolution	LROC	Provide uncontrolled illumination movies, 1 each of north and south lunar poles over the course of 1 lunar year at an average time resolution of 5 hours or better (Wide Angle Camera)
	LROC	Provide meter scale resolution summer (uncontrolled) mosaics of the lunar poles ($\pm$4 degrees) (Narrow Angle Camera)
	LOLA	Polar region maps of latitudes 86°–90° with a vertical resolution of 10 cm and a spatial resolution of 35 m or better after one year
	DLRE	Provide polar illumination map at better than 500 m spatial scales over a full diurnal cycle
The LRO shall characterize lunar mineralogy by measuring UV, visible, and infrared spectral differences and variations at km scales globally	LROC	Global imaging 400 m/pixel in the ultraviolet bands and 100 m/pixel in the visible bands, ten uncontrolled demonstration multi-spectral mosaics for high priority targets
	DLRE	Global fine-component thermal inertia, silicate mineralogy and Lambert albedo from thermal emission, solar reflectance and topography measurements with greater than 50% spatial coverage at the equator
The LRO shall perform hydrogen mapping with a sensitivity of 100 ppm or better, a SNR of 3, and 10 km resolution in the polar regions	LEND	Determine hydrogen content of the subsurface at the polar regions with spatial resolution of 10 km and with sensitivity to concentration variations of 100 parts per million at the poles

3 Mini Radio-Frequency Technology Demonstration

The Mini-RF system has been included in the LRO payload through multi-agency agreements and sponsorship. Its primary purpose is technical demonstration in the lunar environment of a unique miniaturized multi-mode radar observatory. Its synthetic aperture radar (SAR) imaging modes are most relevant to the scientific and exploratory roles of LRO. The mini-RF SAR baseline modes include: two frequencies—S-band (13 cm) and X-band (4 cm); two resolutions—baseline (150 m/75-m pixels) and zoom (15 m/7.5-m pixels); and dual-polarization—transmit on one and receive on like and orthogonal polarizations. The nominal incidence is 45° side-looking; swath widths vary by mode from ∼4 km to ∼6 km. The primary data products will be multi-mode Stokes parameters (or their primitives), which will be a major step forward in space-based radar astronomy (Raney 1998, 2006). In addition, there is an experimental two-pass interferometric mode (single polarization), and the possibility of bistatic radar experiments. The instrument mass is about 12 kg, and the antenna measures 1.8 m long and 0.6 m high.

Radar is an effective methodology in the exploration of lunar and planetary water-ice deposits (Ostro 2002; Campbell et al. 2005; Stacy 1993; Stacy and Campbell 1993). Data from Earth-based observations (such as from the Arecibo radio telescope), as well as from spacecraft, have provided evidence that large and very cold deposits of ice (as occur on Jupiter's moon Europa, or in the polar regions of Mercury) have unique radar reflective properties. Traditionally, these measurements have been based on the received powers observed respectively on the like- and the opposite-sense polarizations in response to circularly polarized transmitted signals. The total power P_{T} is the sum of the two received powers. The power ratio of the same-sense polarization to the opposite-sense polarization is known as the circular polarization ratio (CPR). Both P_{T} and CPR are relatively large when reflected from volumetric deposits of water-ice, in contrast the weaker reflections from a dry planetary surface. The enhanced returns can be explained by the coherent backscatter effect, which occurs when reflections within the volume of the ice reinforce reflections from the top surface (Peters 1992). The effect is pronounced for relatively pure presentations, such as on Europa, for which $P_{\mathrm{T}} + \mathrm{CPR} \sim 4$. The effect would be subdued for less pure ice that may lie beneath a layer of lunar regolith. In addition to the like- and cross-polarized images, the Mini-RF imaging mode will include the complex cross-product between the two polarizations. The resulting data will be sufficient to calculate the four Stokes' parameters across the imaged field, which will be a major innovation for radar of this class, thus enhancing the technology demonstration as well as the exploratory aspects of this instrument.

One bistatic radar measurement is available from the Clementine mission that suggests the presence of water-ice at the south pole of the moon (Nozette et al. 1996, 2001; Lichtenberg 1996), although the data are far too limited to be conclusive. These limitations include: unfavorable low-incidence, only one frequency, relatively coarse resolution, low signal-to-noise ratio, lack of radiometric calibration, and incoherence. The Mini-RF instrument is designed to overcome these limitations.

Operations over the lunar polar regions (above 80° latitude) are the main areas of intended operation. There are several reasons for this: 1) the lunar polar mapping anticipated from the Forerunner S-band SAR, the Mini-RF prototype, which is a guest payload from the United States to the 2008 Chandrayaan mission of India; 2) opportunities for frequent multi-pass coverage to provide bases for comparison across the Mini-RF modes; and 3) the increased likelihood of covering potential water-ice in the cold traps. Initial planning includes dedicated data takes sufficient to demonstrate the various radar modes. It is expected

further into the mission that additional operational time will be allotted to the mini-RF instrument, on a non-interference basis with the main LRO payload instruments, to collect data of scientific value over selected sites on the lunar surface.

4 LRO Mission Design and Spacecraft

The Lunar Reconnaissance Orbiter is designed for a one-year base mission with a goal of an extended mission of up to four additional years. LRO will be launched on an Atlas 5 401 Launch Vehicle (Fig. 12) along with its companion spacecraft, the Lunar CRater Observation and Sensing Satellite (LCROSS), into a direct insertion trajectory to the Moon (Fig. 13). The on-board mono-propellant hydrazine propulsion system will be used to capture into a polar orbit at the Moon, timed to obtain an orbit plane that enables optimum lighting conditions in polar regions during summer and winter seasons. Additional burns will circularize the orbit and maintain it during the base mission at an altitude of 50 ± 20 km. A lower-maintenance, elliptical orbit of 30×216 km will be used for commissioning and may be used for the extended mission. The spacecraft carries enough fuel to provide over 1300 m/s of velocity change (delta V) for orbit capture and maintenance.

The orbiter is a 3-axis stabilized, nadir-pointed spacecraft, designed to operate continuously during the primary mission (Figs. 14 and 15). Four reaction wheels provide attitude

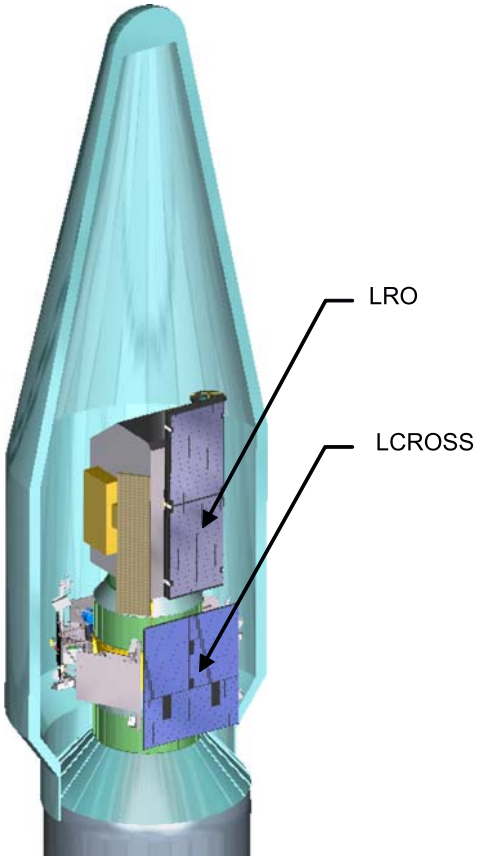

Fig. 12 LRO in Launch Fairing above its companion spacecraft LCROSS

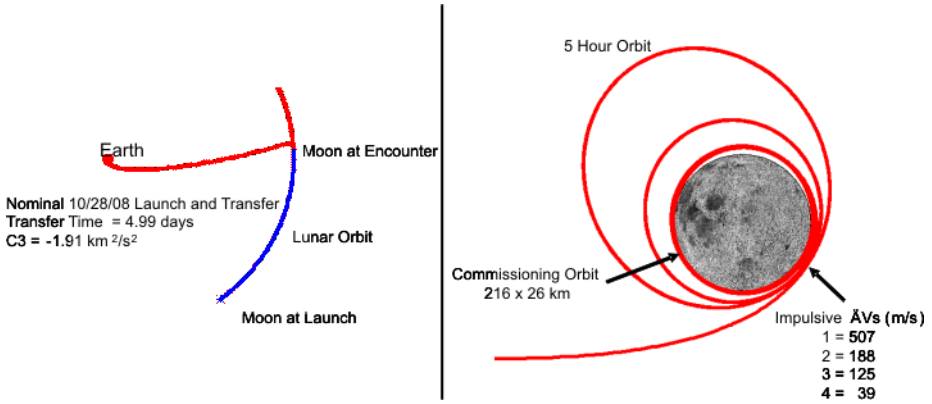

Fig. 13 LRO will have a four to five day cis-Lunar transfer trajectory with orbital insertion into the final mapping orbit using several impulsive maneuvers to obtain a polar orbit

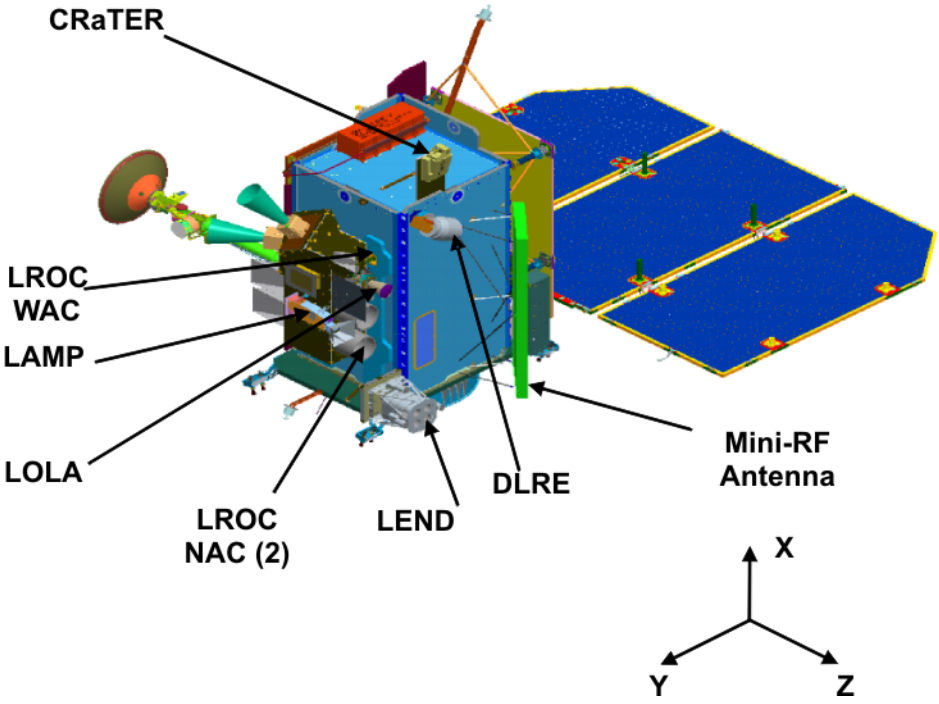

Fig. 14 The LRO instrument suite will be accommodated on an instrument deck and on the body of the LRO spacecraft. The rigid solar arrays are shown deployed. All instrument fields of views are aligned in the nadir ($+z$) direction

control to 60 arc sec and momentum storage of up to 2 weeks, with thrusters providing momentum dumping once per month. Two star trackers and an inertial reference unit provide attitude knowledge of 30 arc sec. Coarse sun sensors provide attitude information in con-

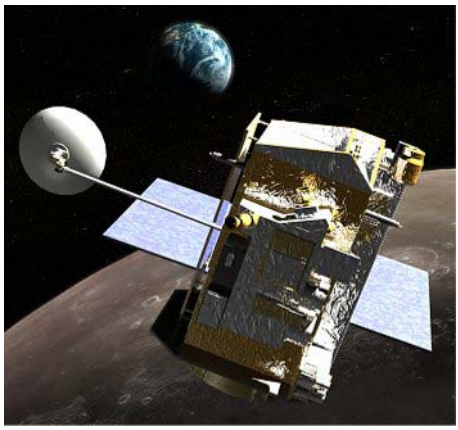

Fig. 15 Artist conception of LRO spacecraft in lunar orbit

Table 7 LRO instrument mass and power allocations

Instrument	Mass allocation (kg)	Power orbit average allocation (W)
CRaTER	6.4	5.9
DLRE	11.9	21.6
LAMP	5.3	4.86
LEND	23.7	13.0
LOLA	15.3	39.6
LROC	16.5	27.6
Mini-RF	12.6	11.2

tingency modes, to enable and maintain proper attitude with respect to the sun, keeping the spacecraft power positive and thermally stable.

A 10.7 square meter solar array provides 1850 W end-of-life during the sunlit portion of the orbit. An 80 A-hr lithium-ion battery maintains the bus voltage and provides operational power during the orbit eclipses and survival power during the rare, long eclipses of the sun by the earth. The power electronics distributes the raw 28 ± 7 V to the instruments and the spacecraft bus electronics, delivering over 800 W average power each orbit.

The flight computer is a RAD-750 processor executing at 133 MHz. Two 100 Gbyte recorders store science data for playback to the earth at 100 Mbps through a 40 W Ka-band transmitter and high-gain antenna. An S-band system provides command, engineering telemetry, and navigation functions. Laser ranging capability provides $\sim$10 cm position precision during four one-hour passes per day. This data, when combined with lunar measurements from LOLA, will improve the orbit determination capability of LRO.

The thermal control system utilizes heat pipes to spread heat and move it to the zenith-facing radiators. A modular structure design enables parallel assembly of the spacecraft.

The total mass of the observatory is less than 949 kg dry and 1846 kg fully fueled; Instrument mass and power allocations are shown in Table 7.

Acknowledgements We would like to thank the Ames Robotic Lunar Exploration Program Office, the Marshall Lunar Precursor Robotic Program Office, the LRO Project Team, the NASA Headquarters Exploration Systems Mission Directorate, and the NASA Headquarters Science Mission Directorate for their

contributions and support in coordinating this effort. We would also like to especially acknowledge the contributions of Kristina Safdie in organizing and putting this manuscript in its final form.

Appendix

Table 8 List of acronyms

AO	Announcement Of Opportunity
C&DH	Command & Data Handling
CPR	Circular Polarization Ratio
CRaTER	Cosmic Ray Telescope For The Effects Of Radiation
CTX	Context Camera
DDL	Double-Delay Line
DLRE	Diviner Lunar Radiometer Experiment
FOV	Field-Of-View
GCR	Galactic Cosmic Rays
HEND	High Energy Neutron Detector
ISIS	Software For Imagers And Spectrometers
LEND	Lunar Exploration Neutron Detector
LET	Linear Energy Transfer
LOLA	Lunar Orbiter Laser Altimeter
LPRP	Lunar Precursor Robotic Program
LRO	Lunar Reconnaissance Orbiter
LROC	Lunar Reconnaissance Orbiter Camera
LCROSS	Lunar CRater Observation and Sensing Satellite
MARCI	Mars Color Imager
MRO	Mars Reconnaissance Orbiter
MCP	Microchannel Plate
Mini-RF	Mini Radio Frequency
NAC	Narrow Angle Camera
OAP	Off-Axis Paraboloidal
ppm	Parts Per Million
PSR	Permanently Shadowed Region
SAR	Synthetic Aperture Radar
SBE	Surface Boundary Exosphere
SCS	Sequencing And Compressor System
SEP	Solar Energetic Protons
SNR	Signal To Noise Ratio
SOC	Science Operations Center
SPE	Solar Particle Event
TEP	Tissue Equivalent Plastic
WAC	Wide-Angle Camera

References

D.B. Campbell, L.M. Carter et al., in *Workshop on Radar Investigations of Planetary and Terrestrial Environments*, Houston, TX, vol. 6026 (2005)

E.M. Eliason, A.S. McEwen, M.S. Robinson, E.M. Lee, T. Becker, L. Gaddis, et al., in *Abstracts of 30th Lunar Planetary Sciences Conference, abstract 1933* (1999)

W.C. Feldman et al., Science **281**, 1496 (1998)

W.C. Feldman et al., J. Geophys. Res. E2 **105**(1), 4125 (2000)

C.L. Lichtenberg, *Bistatic Radar Observations of the Moon Using the Clementine Spacecraft and Deep Space Network*, Ph.D. Thesis (1996)

M.C. Malin et al., J. Geophys. Res. **106**, 17651 (2001)

D. McCleese, J. Schofield, F. Taylor, S. Calcutt, M. Foote, D. Kass, et al., J. Geophys. Res. (2007, in press)

A.E. Metzger, J.I. Trombka, L.E. Peterson et al., Science **179**, 800 (1973)

I.G. Mitrofanov et al., Science **297**, 78 (2002)

S. Nozette, C.L. Lichtenberg, P. Spudis, R. Bonner, W. Ort, M. Robinson, E.M. Shoemaker, Science **274**, 1495 (1996)

S. Nozette, M.S. Spudis, D.B.J. Robinson, C. Bussey, R. Bonner, J. Geophys. Res. **106**(10), 23253 (2001)

S.J. Ostro, in *The Encyclopedia of Physical Science and Technology*, 3rd edn., ed. by R.A. Meyers (Academic, Orlando, 2002) p. 12295

K.J. Peters, Phys. Rev. Revis. B **46**, 801 (1992)

R.K. Raney, in *Principles and Applications of Imaging Radar*, ed. by F. Henderson, A. Lewis (Wiley, New York, 1998), p. 9

R.K. Raney, *Hybrid-Polarity SAR Architecture*. CD-ROM Proceedings. IEEE International and Geoscience Remote Sensing Symposium IGARSS, Denver, CO (2006)

D.E. Smith et al., J. Geophys. Res. **106**(E10), 23689 (2001)

S.C. Solomon et al., Planet. Space Sci. **49**, 1445 (2001)

D.C. Slater, S.A. Stern, T. Booker, J. Scherrer et al., in *UV/EUV and Visible Space Instrumentation for Astronomy and Solar Physics*, ed. by O.H.W. Siegmund, S. Fineschi, M.A. Gummin, Proceedings of SPIE, vol. 4498 (2001), pp. 239

N.J.S. Stacy, *High-Resolution Synthetic Aperture Radar Observations of the Moons* (Cornell University, Ithaca, 1993), p. 210

N.J.S. Stacy, D.B. Campbell, in *Proceedings IEEE Geoscience and Remote Sensing Symposium IGARSS93*, Tokyo, Japan (1993), p. 30

S.A. Stern, J.R. Scherrer, D.C. Slater, G.R. Gladstone, L.A. Young, G.J. Dirks, J.M. Stone, M.W. Davis, in *X-Ray, UV, Visible, and IR Instrumentation for Planetary Missions*, ed. by O.H.W. Siegmund, G.R. Gladstone. Proceedings of SPIE, vol. 5906B (2005)

S.A. Stern, Rev. Geophys. **37**, 453 (1999)

A.P. Vinogradov et al., Space Res. (Russ.) **4**, 871 (1966)

R.R. Vondrak, LPI Contrib. **652**, 246 (1988)